

RESEARCH PAPER

# CPK3-phosphorylated RhoGDI1 is essential in the development of *Arabidopsis* seedlings and leaf epidermal cells

Yuxuan Wu<sup>1,2</sup>, Shujuan Zhao<sup>1,2</sup>, Han Tian<sup>3</sup>, Yuqing He<sup>1,2</sup>, Wei Xiong<sup>1,2</sup>, Lin Guo<sup>3</sup> and Yan Wu<sup>1,2,\*</sup>

<sup>1</sup> State Key Laboratory of Hybrid Rice, College of Life Sciences, Wuhan University, Wuhan 430072, China

<sup>2</sup> Department of Cell and Developmental Biology, College of Life Sciences, Wuhan University, Wuhan 430072, China

<sup>3</sup> Department of Biochemistry, College of Life Sciences, Wuhan University, Wuhan 430072, China

\* To whom correspondence should be addressed. E-mail: [wuy@whu.edu.cn](mailto:wuy@whu.edu.cn)

Received 12 February 2013; Revised 15 May 2013; Accepted 20 May 2013

## Abstract

The regulation of Rho of plants (ROP) in morphogenesis of leaf epidermal cells has been well studied, but the roles concerning regulators of ROPs such as RhoGDIs are poorly understood. This study reports that AtRhoGDI1 (GDI1) acts as a versatile regulator to modulate development of seedlings and leaf pavement cells. In mutant *gdi1*, leaf pavement cells showed shorter lobes in comparison with those in wild type. In *GDI1-14* seedlings (*GDI1*-overexpression line) the growth of lobes in pavement cells was severely suppressed and the development of seedlings was altered. These results indicate that GDI1 plays an essential role in morphogenesis of epidermal pavement cells through modulating the ROP signalling pathways. The interaction between GDI1 and ROP2 or ROP6 was detected in the leaf pavement cells using FRET analysis. Dominant negative, not constitutively active, *DN-rop6* could weaken the effect caused by overexpression of *GDI1*; because the pleiotropic phenotype of *GDI1-14* plants was eliminated in the hybrid line *GDI1-14 DN-rop6*. GDI1 could be phosphorylated by CPK3. Three conserved Ser/Thr residues in GDI1 were determined as targeted amino acids for CPK3. Overexpression of *GDI1(3D)*, not *GDI1(3A)*, could rescue the abnormal growth phenotypes of *gdi1-1* seedlings, demonstrating the impact of GDI1 phosphorylation in the development of *Arabidopsis*. In summary, these results suggest that GDI1 regulation in morphogenesis of seedlings and leaf pavement cells could be undergone through modulating the ROP signalling pathways and the phosphorylation of GDI1 by CPK3 was required for the developmental modulation in *Arabidopsis*.

**Key words:** Calcium, CPK3, GDI1, pavement cells, phosphorylation, ROP.

## Introduction

The ROP (Rho of Plants) proteins are essential molecules in divergent developmental processes, such as tip growth in pollen tubes, hair elongation in roots, and pavement cell development in leaves (Fu and Yang, 2001; Fu *et al.*, 2005; Klahre and Kost, 2006; Xu *et al.*, 2010). Acting as versatile regulators, ROP signalling is modulated through transition between states of inactive GDP-bound and active GTP-bound while responding to diverse extracellular stimuli (Fu and Yang, 2001; Wu *et al.*, 2001; Lavy *et al.*, 2007). The activity of ROPs is regulated by GDP dissociation inhibitors (RhoGDIs), guanine nucleotide

exchange factors (GEFs) and GTPase-activating proteins (GAPs). GEFs activate Rho GTPases which are released by GDIs in cytoplasm through promoting exchange of GDP to GTP in Rho GTPases (Berken *et al.*, 2005; Kaothien *et al.*, 2005; Gu *et al.*, 2006; Basu *et al.*, 2008). GAPs control the ability of Rho GTPases to hydrolyse GTP to GDP which facilitate reinstatement of Rho GTPases in GDP-bound (Wu *et al.*, 2000; Klahre and Kost, 2006; Hwang *et al.*, 2008).

GDIs sequester GDP-bound soluble fractions of Rho GTPases in cytoplasm and inhibit spontaneous dissociation

Abbreviations: GAP, GTPase-activating protein; GDI, GDP dissociation inhibitor; GEF, guanine nucleotide exchange factor;.

© The Author [2013]. Published by Oxford University Press [on behalf of the Society for Experimental Biology].

This is an Open Access article distributed under the terms of the Creative Commons Attribution Non-Commercial License (<http://creativecommons.org/licenses/by-nc/3.0/>), which permits non-commercial re-use, distribution, and reproduction in any medium, provided the original work is properly cited. For commercial re-use, please contact [journals.permissions@oup.com](mailto:journals.permissions@oup.com)

of GDP from Rho GTPases (Kost, 2008). Three members of RhoGDI homologues, AtRhoGDI1, AtRhoGDI2a, and AtRhoGDI2b have been identified in the *Arabidopsis* genome (Bischoff *et al.*, 2000). It has been demonstrated that the AtRhoGDI1 (GDI1) may interact with ROP4 or ROP6 *in vitro* (Bischoff *et al.*, 2000). The GDI1 plays essential role in root hairs growth through controlling activity of NADPH oxidase RHD2/AtRbohC in *Arabidopsis* (Carol *et al.*, 2005). Coexpressing *GDI1* and *ROP1* in tobacco pollen tubes reduces formation of transverse actin bundles (Fu *et al.*, 2001). In addition, deficiency in *GDI2a* leads to depolarization of a pollen tube growth (Hwang *et al.*, 2010). Tobacco NtRhoGDI2 mediates recycling of NtRac5 from the flanks of the tip to the apex of a pollen tube while maintaining the polarized ROP signalling in pollen tubes (Klahre *et al.*, 2006). Although the regulation of GDIs in the polar growth of root hairs and pollen tubes is well studied, the involvement of GDIs in other developmental processes, such as seedling development, is poorly understood.

In *Arabidopsis*, ROP signalling pathways are involved in an assortment of developmental aspects, including polar growth of pollen tubes, elongation of root hairs, morphogenesis of leaf pavement cells, and the response to a plant hormone signal (Lemichez *et al.*, 2001; Baxter-Burrell *et al.*, 2002; Fu *et al.*, 2005; Wong *et al.*, 2007; Yang, 2008; Xu *et al.*, 2010). Elegant studies have demonstrated that interdigitating growth between adjacent pavement cells of *Arabidopsis* is precisely regulated by the plant hormone auxin. (Fu *et al.*, 2005, 2009; Xu *et al.*, 2010). Coordination of ROP2 and Rop-interactive CRIB motif-containing protein 4 (RIC4) promotes outgrowth of lobes through diffusely assembling cortical actin microfilaments (Fu *et al.*, 2005), whereas collaboration of ROP6 and RIC1 suppresses lobes outgrowth through organizing microtubules (Fu *et al.*, 2009).

The regulation of a RhoGDI by phosphorylation modification is critical for GDI function and has an impact to the binding ability of a GDI with a Rho GTPase in mammalian cells (Dransart *et al.*, 2005). The mammalian RhoGDI1 is phosphorylated at two serine residues (Ser101 and Ser174) by PAK1 (p21-activated kinase 1) upon EGF stimulation, which promotes specific release of Rac1, indicating the key role of GDI1 phosphorylation in delivering Rac1 in mammalian cells (DerMardirossian *et al.*, 2004). However, the dissociation of a ROP protein from the ROP-GDI complex in plant cells has not been reported, and whether GDIs perform as upstream players for ROPs in the regulation of epidermal cell growth is elusive.

This study reports that the AtRhoGDI1 (GDI1) acts as a vital regulator in development of seedlings and morphogenesis of leaf pavement cells in *Arabidopsis*. The interaction between GDI1 and ROP2 or ROP6 was detected in leaf pavement cells. In addition, dominant negative GDP-bound *rop6* (*DN-rop6*) could rescue the phenotypes caused by *GDI1* overexpression. Phosphorylation of GDI1 by CPK3 could be crucial for interactions of GDI1-ROP2 as well as GDI1-ROP6. The results suggest that GDI1 regulation is essential for a developing pavement cell. Phosphorylation of CPK3 on GDI1 may be a key step in the morphogenesis of pavement cells in *Arabidopsis*.

## Materials and methods

### Plant materials and growth conditions

The mutant *gdi1-1* (SALK\_129991) was obtained from ABRC ([www.arabidopsis.org/abrc](http://www.arabidopsis.org/abrc)) and homozygous plants were identified with the protocol described by Alonso *et al.* (2003). Mutant *scn1* alleles (*scn1-1*, *scn1-2*, and *scn1-3*) were kindly provided by Dr Liam Dolan (John Innes Centre, Norwich, UK). Surface-sterilized seeds of *Arabidopsis thaliana* were grown on Murashige and Skoog plates (PhytoTechnology, USA) containing 1% (w/v) sucrose and 0.8% (w/v) agar. After 2 days of stratification at 4 °C, they were transferred to a growth chamber for germination, under a 16h/8h light/dark cycle at 23 °C.

### Morphometry analysis for pavement cells

The morphometry analysis for pavement cells was performed following methods described previously (Fu *et al.*, 2005; Le *et al.*, 2006; Sorek *et al.*, 2011; Zhang *et al.*, 2011). Briefly, pavement cells in one-third of the apical regions of 7-day-old cotyledons were selected for the morphometry analysis. The cotyledons were stained with propidium iodide, and then pavement cells in abaxial epidermis were imaged using confocal laser scanning microscopy (FV1000, Olympus, Japan). The lobe length of pavement cells was quantified using MetaMorph 7.5 software (Molecular Devices, USA). Over 100 cells from five independent cotyledons were measured in each independent experiment. The analytic method has been described previously (Fu *et al.*, 2005). The area and perimeter were measured with ImageJ software (version 1.44, <http://rsb.info.nih.gov/ij/>). According to the protocol that was described in several reports (Fu *et al.*, 2005; Le *et al.*, 2006; Sorek *et al.*, 2011; Zhang *et al.*, 2011), the circularity of a pavement cell is defined by calculating  $4\pi$  area/perimeter<sup>2</sup> (Sorek *et al.*, 2011). In order to quantify the number of skeleton ends of a pavement cell, the region of a pavement cell was outlined and filled with ImageJ software; then the processed image was copied and pasted as a new image. Subsequently it was analysed with the 'plugin in' of 'skeleton' embedded in ImageJ, which calculates the number of skeleton ends. Each experiment was repeated at least for three times, and the pairwise T-tests were performed for all comparisons to determine the *P*-values.

### FRET analysis

One-week-old cotyledons from hybrid plants of *GDI1-YFP*, *CFP-ROP2*, and *GDI1-YFP CFP-ROP6* (CFP, cyan fluorescent protein; GFP, green fluorescent protein; YFP, yellow fluorescent protein) were used for fluorescence resonance energy transfer (FRET) analysis. Images were acquired with confocal laser scanning microscopy. The sensitized emission method (Kraynov *et al.*, 2000) was used for the FRET analysis. As for negative controls, pavement cells in transgenic lines expressing *YFP*, *CFP-ROP2*, or *CFP-ROP6* were used. Correction factors were measured by calculating the fluorescent intensity in pavement cells of transgenic plants *CFP-ROP2*, *CFP-ROP6*, or *GDI1-YFP*. First, YFP fluorescent signal was acquired with excitation wavelength setting at 515 nm and emission wavelength setting at 535–600 nm. Then, CFP fluorescence was captured with excitation wavelength setting at 440 nm and emission wavelength setting at 480 nm. The FRET signal was detected with the excitation wavelength setting at 440 nm and emission wavelength setting at 535–600 nm. Raw FRET images and the correction factor were analysed with MetaMorph 7.5 software (Molecular Devices, USA). The bleed-through and background signals were eliminated by calculating the correction factor using MetaMorph 7.5 software; thus the corrected FRET signal was obtained. At final step, FRET efficiency was further calculated using MetaMorph 7.5 software in which the corrected FRET signal was divided by the CFP signal (Yoshizaki *et al.*, 2003). The information about plasmids cloning used for FRET assay can be found in [Supplementary Methods](#) and [Supplementary Tables S1](#) and [S2](#) (available at *JXB* online).

### Pull-down assay

The pull-down assay was performed following the method described previously (Gu *et al.*, 2006; Wang *et al.*, 2011) with minor modifications. Briefly, recombinant His-ROP protein (10 µg) was incubated with GST-GDI1 protein (50 µg) that was already conjugated with glutathione sepharose beads (GE Healthcare, USA) in 500 µl binding buffer (20 mM Tris-HCl, pH 7.5, 150 mM NaCl, 10% glycerol, 0.1% Triton X-100, 5 mM MgCl<sub>2</sub>, 1 mM EDTA) (Gu *et al.*, 2006). After incubation for 1 hour, the beads were washed for five times with binding buffer to remove the unbound protein. The pulled-down protein complex was separated in 10% SDS-PAGE gel and detected by anti-His antibody (Proteintech Group, USA). For semi-*in vivo* pull-down assay, recombinant His-CPK3 protein was purified and conjugated to TALON beads (Clontech, USA), and then incubated with total protein extracted from 2-week-old GDI1-14 plants or 35S:GFP plants. After washing, the pulled-down protein complex was separated in 10% SDS-PAGE gel and detected with anti-GFP antibody (Proteintech Group, USA). GFP-GDI1 protein incubated with TALON beads was used as the control. The reciprocal control was using GFP protein that was pre-incubated with TALON beads and then conjugated with His-CPK3 protein. After five washes with binding buffer, the pulled-down protein complex was separated in 10% SDS-PAGE gel and detected by anti-GFP antibody (Proteintech Group, USA). Information about plasmids used in the pull-down assay is given in [Supplementary Methods](#).

### In vitro kinase assay

The recombinant protein His-CPK3 (kinase) and the substrates GST-GDI1 (full length) and GST-GDI1 fragment (Ser 2 to Asp 57) were purified from *E. coli*. The *in vitro* kinase assay was carried out following the protocol described in previous reports (Boudsocq *et al.*, 2010; Geiger *et al.*, 2010) with minor modifications. The reaction mixture (20 µl) was composed of 1 µg kinase protein (His-CPK3), 10 µg substrate GST-GDI1 (full length or fragment), and the reaction buffer (25 mM Tris-HCl pH 7.4, 12 mM MgCl<sub>2</sub>, 2 mM CaCl<sub>2</sub>, 1 µM ATP, 5 µCi of [ $\gamma$ -<sup>32</sup>P]ATP, 1 mM DTT, 1 mM Na<sub>3</sub>VO<sub>4</sub>, 5 mM NaF). After incubation for 30 minutes at 30 °C, the reaction was stopped by adding the sample buffer and then separated with 10% SDS-PAGE gel. The  $\gamma$ -<sup>32</sup>P radioactivity was detected with Typhoon 9200 phosphorimager (GE Healthcare).

## Results

### The involvement of GDI1 in development of seedlings and leaf epidermal cells

To investigate the role of AtRhoGDIs (GDIs) in a developmental process, this study analysed expression patterns of three *Arabidopsis* GDI homologues, *GDI1*, *GDI2a*, and *GDI2b* using reverse-transcription PCR. Results showed that *GDI1* gene expression was detectable in all tested tissues of *Arabidopsis*. The expression of *GDI2a* and *GDI2b* was, however, predominantly showed in tissues of inflorescences and flowers ([Supplementary Fig. S1A](#)). Hence, this study attempted to explore GDI1 function in the seedling development. While analysing the T-DNA insertion mutant *gdil-1* (SALK\_129991), it was found that expression level of *GDI1* in mutant *gdil-1* was declined significantly ([Supplementary Fig. S1B, C](#)). The root hair growth in *gdil-1* seedlings was arrested ([Supplementary Fig. S1D](#)), which was similar to the phenotype observed in the study

about *scn1* mutant alleles (Carol *et al.*, 2005). Initially it seemed that the aberrant root hair growth in *gdil-1* mutant was rescued by the YFP-tagged GDI1 fusion protein ([Supplementary Fig. S1D](#)), implying the importance of GDI1 in root hair growth. In addition, it was also noticed that transgenic plants carrying overexpressed *GDI1* (with or without fluorescent protein-tagging) developed differently from those in *gdil-1* and wild-type Col-0 (WT) ([Fig. 1A](#), [Supplementary S1E](#)). Although curly, narrowed cotyledons and true leaves were occurred in seedlings carrying overexpressed *GDI1* ([Fig. 1A](#), [Supplementary S1E, F](#)), the adult plants with overexpressed *GDI1* could produce normal inflorescences and set seeds. Therefore, this study focused on exploring the influence of GDI1 in the stage of seedling development.

Several independent transgenic lines possessing higher expression level of *GDI1* ([Supplementary Fig. S1C](#)) were selected for subsequent analysis. As for comparisons, transgenic plants carrying GFP-tagged *GDI2b* were also generated ([Supplementary Fig. S1E, G](#)). Notably, seedling growth of transgenic lines with overexpressed *GDI2b* showed normal ([Supplementary Fig. S1E](#)). Together, these results suggest that the diversified seedling growth in transgenic lines with overexpressed *GDI1* or *GDI2b* might be attributed to the divergence of sequence properties in GDI1 and GDI2b proteins. In fact, the N-terminal domain of GDI1 is rather unique than those contained in GDI2b and GDI2a protein sequences ([Supplementary Fig. S2](#)). With such a unique N-terminus, GDI1 might manifest its specific regulation in the development of *Arabidopsis*.

To explore the internal structure of curly leaves occurred in *GDI1* transgenic plants the traverse sections of leaves from *GDI1-14* seedlings were investigated. Results showed that mesophyll cells in leaves of *GDI1-14* seedlings were 'swollen' ([Fig. 1B](#)) and the shape of a leaf epidermal pavement cell was greatly altered, such as that the well-organized interlocking lobe-neck appearance (Fu *et al.*, 2005; Xu *et al.*, 2010) was strictly disturbed ([Fig. 1C, D](#)). The growth phenotypes of *GDI1-14* plants and other transgenic lines carrying different forms of fluorescent protein-tagged *GDI1* fusion constructs were further analysed. Despite which kind of fluorescent tag was fused to GDI1, overexpression of *GDI1*, not *GDI2b*, could alter morphology of epidermal pavement cells in leaves ([Supplementary Fig. S1H](#)). Consequently, attention was turned to characterize the role of GDI1 in development of leaf pavement cells.

The shape of leaf pavement cells was quantitatively analysed among plants of WT, *gdil-1* and *GDI1-14* using the method of geometric analysis (Le *et al.*, 2006; Sorek *et al.*, 2011; Zhang *et al.*, 2011). In order to compare the results from *gdil-1*, the *scn1* mutant alleles (*scn1-1*, *scn1-2*, and *scn1-3*) (Carol *et al.*, 2005) were also analysed. Results indicated that average length of lobes in leaf pavement cells of *gdil-1* and *scn1* was changed with comparison to that in WT ([Fig. 1D](#)). To portray the shape of a pavement cell, the circularity was used as a key parameter which was calculated based on the ratio of perimeter versus area (perimeter/area)



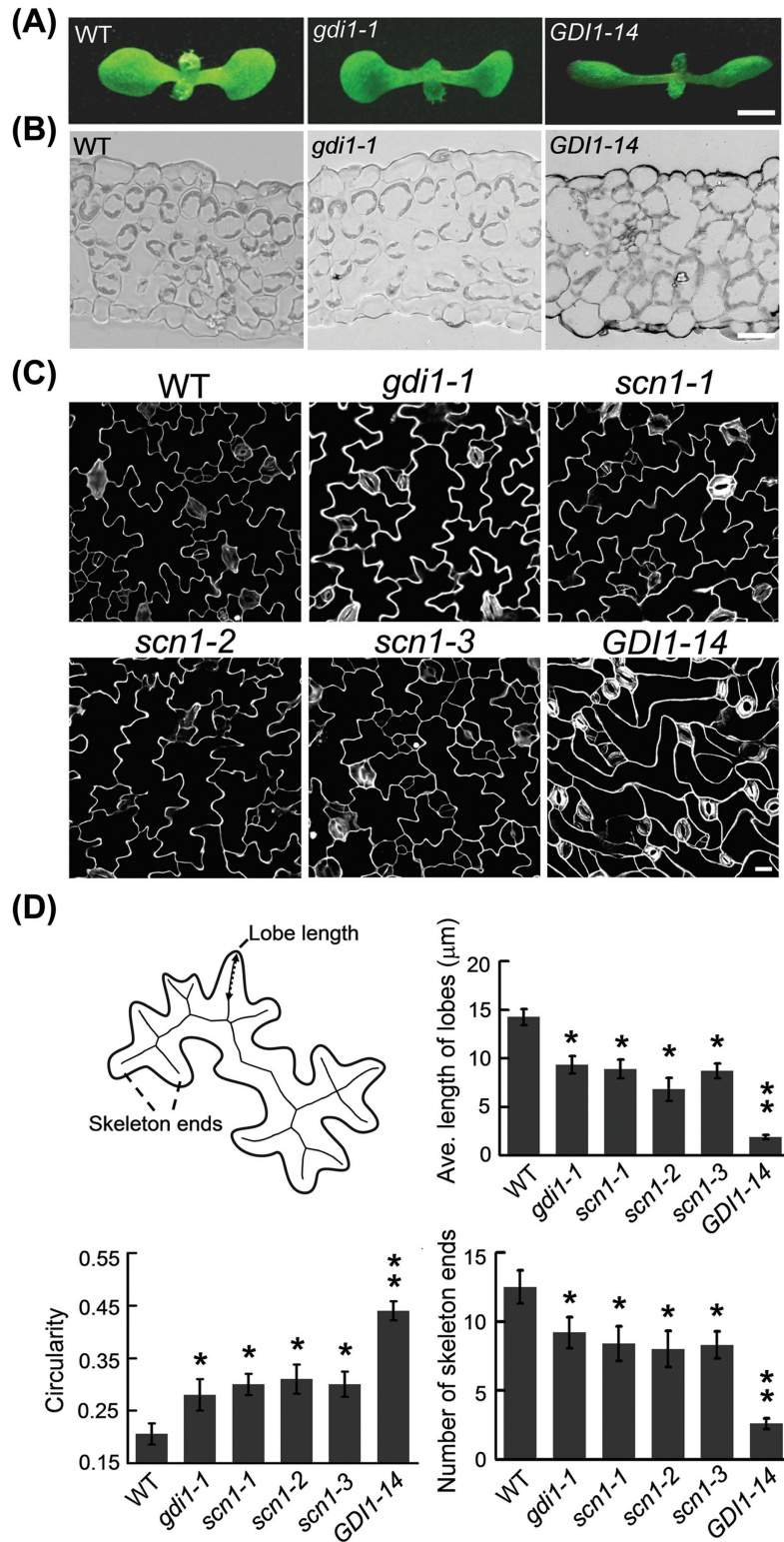


**Fig. 1.** The phenotypes of seedling growth and cell shape in plants of *gdi1* and *GDI1-14*. (A) A 7-day-old seedling of transgenic line *GDI1-14* (*GFP-GDI1*) showed narrower and curly cotyledons while comparing to those in seedlings of *gdi1-1* and WT (Col-0); bar, 0.5 cm. (B) Enlarged mesophyll cells showed in true leaves of 3-week-old *GDI1-14* seedlings; bar, 10  $\mu\text{m}$ . (C) In cotyledons of 7-day-old *gdi1-1* and *scn1* mutant alleles the length of lobes of pavement cells (stained by propidium iodide) was shorter than that in WT, and lobes were almost disappeared in pavement cells of *GDI1-14* seedlings; bar, 10  $\mu\text{m}$ . (D) Geometric analysis on morphogenesis of pavement cells in plants of *gdi1-1*, *scn1* alleles and *GDI1-14*; the lobe length, circularity, and number of skeleton ends were measured in the way that is modelled in upper left corner. In *gdi1* mutant alleles or *GDI1-14* plants, pavement cells have shorter lobes, larger circularity values, and less number of skeleton ends in comparison to WT. Data are mean  $\pm$  SE of three independent experiments ( $n = 100$  for each experiment. \* $P < 0.05$ ; \*\* $P < 0.01$ ) (this figure is available in colour at *JXB* online).

(Fig. 1D). If a pavement cell possesses longer and narrower lobes, it has smaller value in circularity, and *vice versa* (Le *et al.*, 2006; Sorek *et al.*, 2011; Zhang *et al.*, 2011). Using the geometric analytic method (Zhang *et al.*, 2011), larger values of circularity for pavement cells in *gdi1-1* and *scn1* alleles were scored, indicating that the lobe length of pavement cells in *gdi1* mutant alleles was shorter than that in WT (Fig. 1D). The lobe length of pavement cells in *GDI1-14* plants was also analysed. Significant larger value of circularity was measured with *GDI1-14* plants (Fig. 1D). Because the number of skeleton ends is also an important parameter to reflect the lobe numbers for a pavement cell (Sorek *et al.*, 2011), the number of skeleton ends in plants of WT, *gdi1* mutant alleles and *GDI1-14* were additionally compared. The results showed that numbers of skeleton ends were quantitatively reduced in plants of *gdi1* mutant alleles and *GDI1-14* (Fig. 1D). Taken together, the data suggest the involvement of GDI1 in the development of leaf pavement cells. Too much or too little GDI1 may lead to aberrant networking of ROP signalling, in turn, to misregulate the morphogenesis of pavement cells.

#### The interaction between GDI1 and ROPs

To determine the correlation between GDI1 and ROPs (such as ROP2 and ROP6) in pavement cells, the interaction between GDI1 and ROP2 or ROP6 was examined. First, recombinant YFP signal was detected by coexpressing *GDI1-YN* and *ROP2-YC* or *ROP6-YC* (YC, C-terminal YFP fragment; YN, N-terminal YFP fragment) in WT mesophyll protoplasts using bimolecular fluorescence complementation assay (BiFC; Walter *et al.*, 2004); similarly, YFP signal was detected respectively in coexpression of *GDI2a-YN* or *GDI2b-YN* and *ROP2-YC* or *ROP6-YC* (Supplementary Fig. S3A). Next, this study analysed the interaction of GDIs (GDI1, GDI2a, and GDI2b) and

several ROPs (ROP2, ROP4, ROP6, ROP10, and ROP11) in WT pavement cells. Except for the coexpression of GDI2a and ROP11, and GDI2b and ROP10, the YFP signal was detectable in all examined coexpressions (Supplementary Fig. S3B). Collectively, these results demonstrate that GDI1 can interact with multiple ROPs in the pavement cell, which may function via modulation of the entire ROPs network. ROP2 and ROP6 play essential roles in pavement cell development (Fu *et al.*, 2005, 2009; Xu *et al.*, 2010), thus, this study attempted to examine the interaction between GDI1 and ROP2 or ROP6 in leaf pavement cells. The crossed hybrid lines *GDI1-YFP CFP-ROP2* and *GDI1-YFP CFP-ROP6* were analysed using the FRET assay. Not surprisingly, the FRET signal representing the interaction of GDI1 and ROP2 or ROP6 was detected in the plasma membrane and the cell cortex region of pavement cells in leaves from both hybrid lines (Fig. 2, Supplementary Fig. S3C, D). Overall, the results suggest that GDI1 regulation on ROP2 or ROP6 activity may be considered in the development of pavement cells.

To investigate the regulatory relationship between GDI1 and ROP6, the crossed hybrid lines *GDI1-14 ROP6-WT*, *GDI1-14 CA-rop6 (G15V)* and *GDI1-14 DN-rop6 (T20N)* were characterized. While comparing *GDI1-14 ROP6-WT*, normal growth of seedlings and pavement cells was observed in hybrid line *GDI1-14 DN-rop6* (Fig. 3A, B). The data from quantitative analysis indicated that average length of lobes and the number of skeleton ends in pavement cells of *GDI1-14 DN-rop6* seedlings were similar to those in WT seedlings (Fig. 3C), demonstrating that a rescue by *DN-rop6* was incurred in hybrid line *GDI1-14 DN-rop6*. Interestingly, similar growth phenotype in plants of *GDI1-14* and *GDI1-14 CA-rop6* was notable (Fig. 3). These genetic data suggest that introducing *DN-rop6* or *ROP6-WT* into *GDI1-14* could weaken the effect caused by overexpression of *GDI1*; hence, the regulation of GDI1

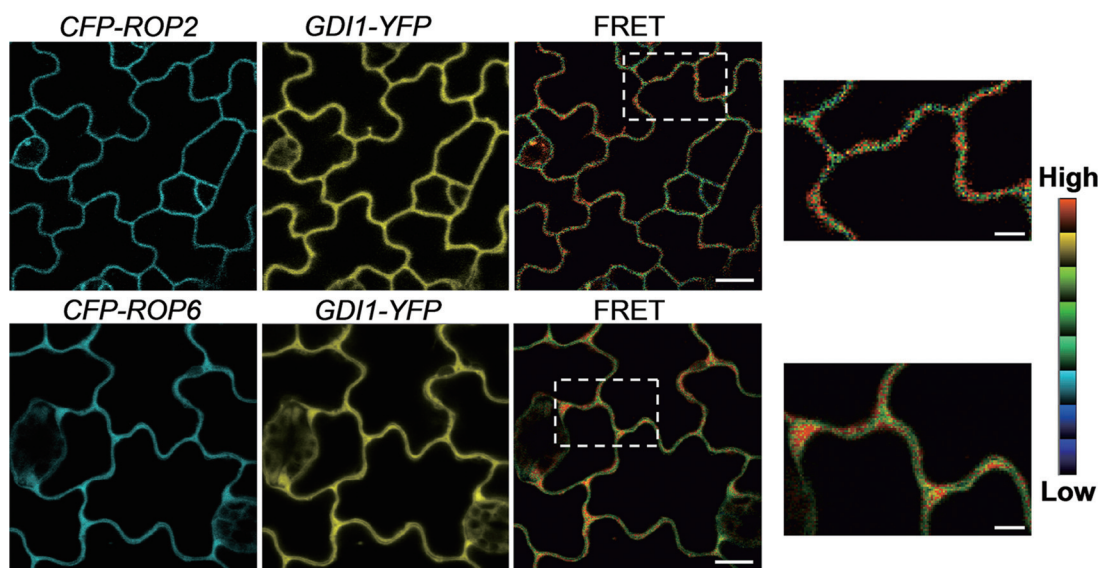


**Fig. 2.** Interaction between GDI1-YFP and CFP-ROP2 (upper panel) or GDI1-YFP and CFP-ROP6 (lower panel) was confirmed with FRET analysis in crossed hybrid lines; bar, 10  $\mu\text{m}$ . Two enlargements show magnified views of FRET signals; bar, 2.5  $\mu\text{m}$ .

in seedling growth and pavement cell development can be mediated by the ROP signalling.

#### Impact of phosphorylation of GDI1 in seedling development

In mammalian cells, phosphorylation status of a RhoGDI is effective in the binding affinity between a RhoGDI and a Rho GTPase (Dransart et al., 2005). The mammalian RhoGDI1 can be phosphorylated by PAK1 at two serine residues (Ser101 and Ser174) upon EGF stimulation and specific

release of Rac1 is then incurred, which indicates the key role of phosphorylation of GDI1 in releasing Rac1 in cytosol (DerMardirossian et al., 2004). To explore the impact of phosphorylation modification of a GDI protein in seedling development, this study performed 2D-gel immunoblotting analysis for the total protein extracted from *GDI1-14* plants. Several acidic forms of GDI1 protein were found (Fig. 4A). The phosphorylated peptides were enriched using the method of immobilized metal ion affinity chromatography (Chen et al., 2011). Three putative amino acids (serine 45, serine 48,

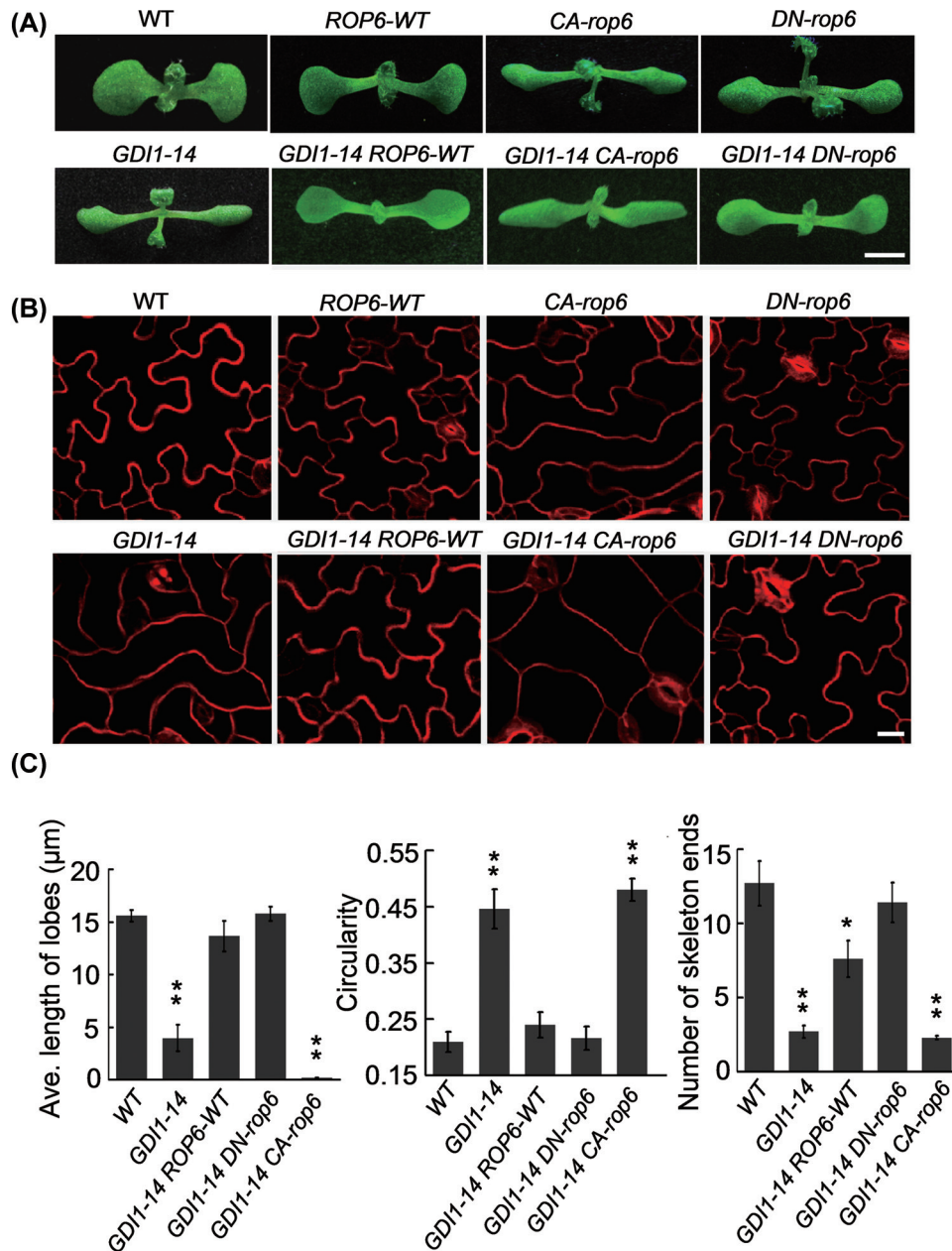


**Fig. 3.** Phenotypes of GDI1 and ROP6 hybrid lines. (A) *CA-rop6* (G15V) seedling showed narrow and curly cotyledons which was similar to *GDI1-14* seedling. Seedlings of hybrid lines *GDI1-14 ROP6-WT* and *GDI1-14 DN-rop6* (T20N) showed normal growth; bar, 0.5 cm. (B) Abnormal morphogenesis of pavement cells in *GDI1-14* seedlings was partially reverted in hybrid lines *GDI1-14 ROP6-WT* and *GDI1-14 DN-rop6*; bar, 10 μm. (C) Geometric analysis on the pavement cells shown in (B). Shorter lobes, larger circularity values, and less number of skeleton ends were scored in *GDI1-14* and *GDI1-14 CA-rop6*. Data are mean ± SE of three independent experiments ( $n = 50$  for each experiment; \* $P < 0.05$ ; \*\* $P < 0.01$ ).



and threonine 52) near the N-terminus of GDI1 were determined (Fig. 4B, Supplementary Fig. S4). To investigate the influence of phosphorylation modification to the binding affinity, the interactions of various forms of GDI1 protein and a ROP protein were analysed. The binding affinity of the

non-phosphorylated form GDI1(3A) [GDI1<sup>S45AS48AT52A</sup> (3A)] or the phosphomimetic form GDI1(3D) [GDI1<sup>S45DS48DT52D</sup> (3D)] to His-tagging ROPs (ROP2, ROP6, ROP10) was examined through an *in vitro* pull-down assay. The results showed that GDI1(3D) possessed stronger binding affinity

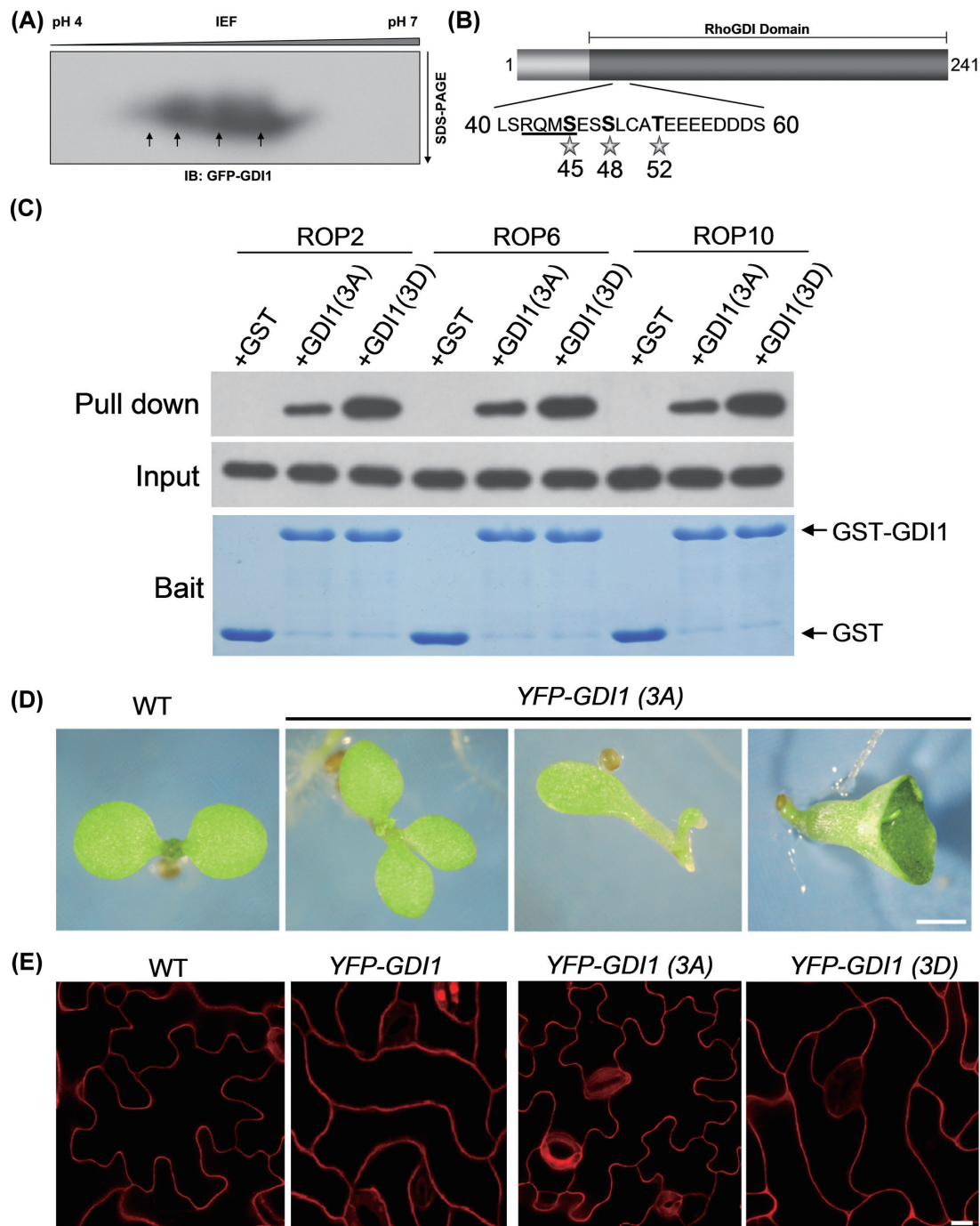


**Fig. 4.** Analysis of GDI1 phosphorylation. (A) Acidic forms of GFP-GDI1 fusion protein (indication of arrows) were detected with 2D gel immunoblotting. (B) Schematic diagram (not scaled) indicating three phosphorylation sites (Ser45, Ser48, and Thr52) in GDI1 protein (RhoGDI domain: 36–241). (C) *In vitro* pull-down assay to confirm the binding affinity between phosphorylated GDI1 and ROPs. The GDI1 phosphomimetic mutant GDI(3D) (S45DS48DT52D) has stronger binding affinity to His-ROPs than the non-phosphorylated mutant GDI(3A) (S45AS48AT52A). Negative control was GST. The loading control of purified GST-tagged GDI1 is shown with Coomassie staining (Bait). His-ROPs were immunoblotted with anti-His antibody (Input). (D) In *GDI1(3A)* transgenic line, 5–15% seedlings displayed abnormal growth of cotyledons (three cotyledons, one cotyledon, or fused cotyledon); bar, 0.5 cm. (E) Overexpressing *GDI1(3A)* did not affect morphogenesis of pavement cells significantly, but overexpression of *GDI1* or *GDI1(3D)* led to severe developmental defects of pavement cells; bar, 10 μm.

to His-tagging ROPs (Fig. 4C), suggesting the importance of phosphorylation status of GDI1 in modulating a ROP protein.

To find out the impact of phosphorylation status of GDI1 in seedling development, transgenic plants carrying plasmid p35S:YFP-GDI1<sup>S45AS48AT52A</sup> (3A) and p35S:YFP-GDI1<sup>S45DS48DT52D</sup> (3D) were characterized (Supplemental Fig. S5). Cotyledon growth in some *YFP-GDI1* (3A) seedlings was severely affected (Fig. 4D), seedlings with three cotyledons or single cotyledon or a ‘cone-shaped’ cotyledon were observed (Fig. 4D, Supplemental Table S3). Interestingly, the shape of mature pavement cells in *YFP-GDI1* (3A) plants was looked normal (Fig. 4E). In sharp contrast, mature pavement cells in leaves of *YFP-GDI1* and *YFP-GDI1* (3D) plants were wholly altered (Fig. 4E). To further confirm the influence of phosphorylation status of GDI1 in seedling development, transgenic lines of *GDI1*, *GDI1* (3D), and *GDI1* (3A) were introduced into *gdi1-1* background respectively; thus, three transgenic lines, *GDI1* (Com), *3A* (Com), and *3D* (Com), were analysed. The development of pavement cells and root hairs in plants of *GDI1* (Com) and *3D* (Com) was recovered to normal growth; however, the recovery was not observed in *3A* (Com) plants (Supplementary Fig. S5). Taken together, these results demonstrate a significant impact of phosphorylation status of GDI1 in development of seedlings and pavement cells in *Arabidopsis*.

#### Phosphorylation of GDI1 by CPK3

Because the consensus sequence R-X-X-S that has been reported as the target domain for calcium-dependent protein kinases (CPKs) (Cheng *et al.*, 2002) is contained in GDI1 protein (Fig. 4B), this study examined the possible phosphorylation modification of CPKs to GDI1. Total 34 CDPKs were determined in *Arabidopsis* (Cheng *et al.*, 2002), among which *CPK3*, *CPK9*, *CPK10*, *CPK28*, and *CPK32* have been reported to possess abundant expression levels in leaves (Boudsocq *et al.*, 2010). This study attested the phosphorylation activities of CPKs on GDI1 and found out that CPK3 could phosphorylate the full length and the peptide fragment of GDI1 protein (Ser 2 to Asp 57) *in vitro* (Fig. 5A). Not surprisingly, a declined phosphorylation level was observed in *GDI1*(3A) (Fig. 5A). Furthermore, this study investigated the interaction between GDI1 and CPK3 and demonstrated the existence of interaction between GDI1 and CPK3 *in vitro* and *in vivo* (Figs. 5B, 5C). To substantiate the involvement of calcium signalling in developing epidermal cells, this study examined the effect of manipulating Ca<sup>2+</sup> release from intracellular calcium stores in the treatment of 2-aminoethyl diphenylborinate (2-APB), an inhibitor of intracellular calcium stores (Engstrom *et al.*, 2002). As results, the average length of lobes of pavement cells in treated WT seedlings was reduced whereas the circularity of pavement cells in treated WT seedlings was increased (Supplementary Fig. S6). Additionally, seedlings were treated with N-(6-aminoethyl)-5-chloro-1-naphthalenesulphonamide hydrochloride (W-7), the calmodulin antagonist that has been used for studying

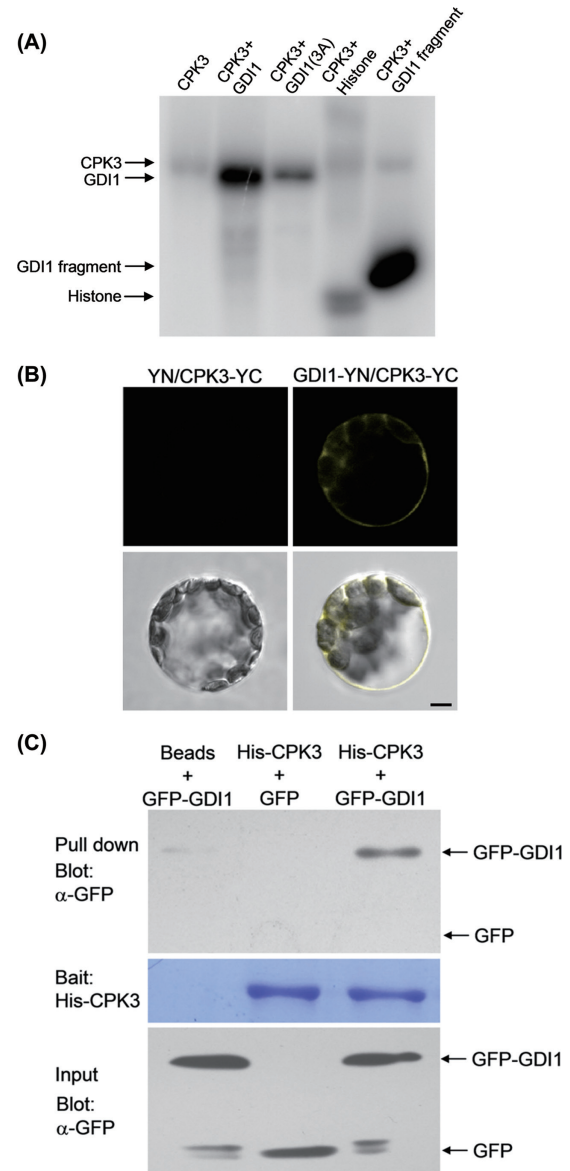


**Fig. 5.** GDI1 phosphorylated by CPK3 *in vitro*. (A) CPK3 phosphorylates GDI1 *in vitro*. Purified His-CPK3 was incubated with GST-GDI1, GST-GDI1<sup>S45AS48AT52A</sup> (3A), Histone (positive control), and GST-GDI1 fragment (Ser 2 to Asp 57) in the presence of [ $\gamma$ -<sup>32</sup>P]ATP respectively. The [ $\gamma$ -<sup>32</sup>P]ATP labelled protein bands are indicated with arrows. (B) Interaction between CPK3 and GDI1 was detected in the BIFC assay (right): YC, C-terminal YFP fragment; YN, N-terminal YFP fragment. Protoplasts expressing pCPK3-YC and vector p35S:YN was used for negative control (left); bar, 5  $\mu$ m. (C) Semi-*in vivo* pull-down assay to confirm the interaction between GDI1 and CPK3. His-CPK3-conjugated TALON beads were incubated with total proteins purified from 2-week-old transgenic plants of *35S:GFP* (control line) and *GDI1-14*. The pulled-down protein complex was detected with anti-GFP antibody. GFP-GDI1 protein incubated with non-conjugated TALON beads (beads+GFP-GDI1) was used for the control. Reciprocally GFP protein incubated with His-CPK3 (His-CPK3+GFP) was also used for the control. The loading control is shown with Coomassie staining (Bait). The input total proteins extracted from *35S:GFP* and *GDI1-14* transgenic plants were immunoblotted with anti-GFP antibody.



CDPKs activities in several reports (Romeis *et al.*, 2000; Kaplan *et al.*, 2006). Notably, the shape of pavement cells in WT cotyledons was obviously altered with treatment (Supplementary Fig. S6). Collectively, these results demonstrate the significance of calcium signalling in the development of pavement cells.

## Discussion

*Diverse regulations of GDI1 to a ROP might exist in Arabidopsis*

RhoGDIs are initially depicted as negative regulators and capable of inhibiting the dissociation of GDP from Rho GTPases in eukaryotic cells (Dransart *et al.*, 2005), which extract the Rho GTPases from plasma membrane to maintain the inactivated Rho GTPases in cytoplasm. Additionally, RhoGDIs can also inhibit the hydrolytic activities of Rho GTPases in mammalian cells (Boulter *et al.*, 2010; Garcia-Mata *et al.*, 2011). RhoGDI1 in mammalian cells is not only able to control stability and homeostasis of multiple Rho GTPases but also acts as a chaperon to facilitate the translocation of Rho GTPases from cytoplasm to the plasma membrane (Boulter *et al.*, 2010). The regulation of RhoGDIs in plant cells, however, is poorly understood. The current study discusses the role of AtRhoGDI1 (GDI1) in modulating the development of *Arabidopsis* seedlings. Overexpression of *GDII* could trigger abnormal growth of seedlings and irregular morphology of leaf epidermal pavement cells, which were similar to those shown in *CA-rop6* transgenic plants. Interestingly, the abnormality of *GDII* transgenic plants can be rescued by *DN-rop6*, not *CA-rop6* (Fig. 3). It is considered that *DN-rop6* might weaken the effect caused by overexpression of *GDII* through binding to excessive amount of GDI1 protein in pavement cells, thereby balancing the interference of overexpressed *GDII*. In a similar fashion, introducing *ROP6-WT* into *GDII* background could also rescue the effect of overexpressed *GDII*. These results suggest the complexity of GDI1 regulation during seedling development. Concerning the shorter lobes shown in abnormally developed pavement cells, a severe phenotype was produced in pavement cells of plants carrying overexpressed *GDII* (Fig. 1). Shorter lobes of pavement cells in plants with positively or negatively modulated ROP activity have been reported previously (Fu *et al.*, 2002). For example, *CA-rop2* and *DN-rop2* play opposite roles in regulating cytoskeleton arrangement; however, expression of these two forms of ROP2 leads to shorter lobes in pavement cells (Fu *et al.*, 2005). The current study hypothesizes that, in addition to playing as the GDP dissociation inhibitor for ROPs, AtRhoGDI1 might take part in stabilizing and distributing ROPs in pavement cells. The results of the interactions of GDI1-ROP2 and GDI1-ROP6 at the cell cortex near the plasma membrane region (Fig. 2) implicate the regulation of GDI1 on the ROP function, which is in agreement with the theory that ROP2 acts mostly at the plasma membrane of lobe region and that ROP6 serves preferentially at the plasma membrane of indentation zone in leaf epidermal pavement cells in *Arabidopsis* (Fu *et al.*,

2002, 2005; Xu *et al.*, 2010). Possibly, during development of leaf pavement cells AtRhoGDI1 could also perform as a chaperon to transport ROP2 to its destination (such as to the cell cortex near lobes) while promoting dissociation of ROP6 from the plasma membrane of the lobe region. Thus, AtRhoGDI1 might possess multiple functions as those that are demonstrated in mammalian cells (Garcia-Mata *et al.*, 2011). In addition, AtRhoGDI1 can regulate multiple ROPs in pavement cells. As tested in this study, except for interacting with ROP2 and ROP6, GDI1 can also interact with ROP4, ROP10, and ROP11. Future studies underlying regulation of the GDI1 in distribution and activity of ROPs in plant cells will provide further insight.

*Phosphorylation of GDI1 by CPK3 implicates convergence of multiple signalling pathways*

The phosphorylation state of RhoGDIs by the protein kinase is a regulatory mechanism for dissociation of Rho GTPases in mammalian cells. The p21-activated kinase 1 (PAK1), a downstream effector of Rac1 and Cdc42, is demonstrated to phosphorylate RhoGDI1 at two amino acids (Ser101 and Ser174) (DerMardirossian *et al.*, 2004). In plant cells, little is known about post-translational modifications of GDIs. This study determined that, CPK3, a calcium-dependent protein kinase, is possible to phosphorylate AtRhoGDI1. Three amino acids, Ser45, Ser48, and Thr52, conserved in GDI1 protein, are key target sites for CPK3. The phosphorylation status of GDI1 influences its binding ability to ROPs. Although the developed pavement cells are looked normal in *GDII(3A)* seedlings, the growth of cotyledons can be severely altered (Fig. 4), which is similar to phenotypes observed in auxin-related mutants (Benková *et al.*, 2003; Jaillais *et al.*, 2007). For example, three cotyledons are observed in mutant *vps29* (vacuolar protein sorting 29) due to disturbed PIN1 polarity (Jaillais *et al.*, 2007). NtRac1 can stimulate expressions of auxin-responsive genes and mediate 26S proteasome-dependent proteolysis of AUX/IAAs proteins (Tao *et al.*, 2002, 2005). In leaf pavement cells, the localization of PIN1 can be affected by the ROP signalling, in turn, the auxin response is subsequently modified (Xu *et al.*, 2010). The current characterization of the transgenic lines *GDII(3A)* and *GDII(3D)* may imply the importance of phosphorylation status of GDI1 in the auxin-regulated developmental processes. A future study to determine the role of GDI1 in auxin polar transport and/or auxin signal transduction may widen the knowledge on this point.

CPK3 is activated in response to salt stress, and it is functional in the ABA-regulated ion channels in guard cells (Mori *et al.*, 2006; Mehlmer *et al.*, 2010). The results of this study suggest a potential role of CPK3 involving in ROP-mediated developmental processes. As an important calcium sensor in plant cells, CPKs have been demonstrated to play diverse roles in modulating polar growth, including root hair growth and pollen tube elongation (Ivashuta *et al.*, 2005; Yoon *et al.*, 2006; Myers *et al.*, 2009). Here it is shown that calcium-mediated signalling in morphogenesis of an epidermal cell may require CPK3-phosphorylated GDI1. Concerning the

functional redundancy (Cheng *et al.*, 2002), the functions of other CPKs in phosphorylation of GDI1 need to be clarified.

Overall, this study provides evidence of a role of GDI1 regulation in the development of seedlings and pavement cells in *Arabidopsis*. The CPK3 phosphorylation of GDI1 may confer a fresh insight to further understand the convergence of extracellular signalling and intracellular ROP signalling pathways, including calcium-dependent modulations.

## Supplementary material

Supplementary data are available at *JXB* online.

**Supplementary Fig. S1.** Characterization of expression patterns of *GDI* genes and phenotypes of *GDI1* transgenic plants.

**Supplementary Fig. S2.** Sequence comparisons of GDIs homologues.

**Supplementary Fig. S3.** Analysis of interactions between GDIs and ROPs.

**Supplementary Fig. S4.** Determination of phosphorylation sites of GDI1 protein.

**Supplementary Fig. S5.** Characterizations of *GDI1* transgenic lines carrying mutated phosphorylation sites.

**Supplementary Fig. S6.** Analysis on effects of calcium level and CPK activity in pavement cell morphogenesis.

**Supplementary Table S1.** Plasmids used in this study.

**Supplementary Table S2.** Primer sequences for *gdi1-1* homozygote (HM) identification, plasmids construction, and reverse-transcription PCR.

**Supplementary Table S3.** Quantitative analysis on cotyledon phenotypes in *YFP-GDI1(3A)* transgenic lines.

Supplementary methods.

## Acknowledgements

The authors thank the Wu lab members for technique help and helpful comments on the manuscripts. They are grateful to Dr Liam Dolan (John Innes Centre, Norwich, UK) for providing *scn1-1*, *scn1-2*, and *scn1-3* seeds, Dr Nam-Hai Chua (Rockefeller University, USA) for providing the plasmid pBA002, and Syngenta for providing the Friendly Laboratories Scholarship to Yuxuan Wu. This work was supported by grants to Yan Wu from the National Natural Science Foundation of China (31270333, 90817013) and the Ministry of Science and Technology of China (2013CB126900).

## References

**Alonso JM, Stepanova AN, Lisse TJ, et al.** 2003. Genome-wide insertional mutagenesis of *Arabidopsis thaliana*. *Science* **301**, 653–657.

**Basu D, Le J, Zakharova T, Mallery EL, Szymanski DB.** 2008. A SPIKE1 signaling complex controls actin-dependent cell morphogenesis through the heteromeric WAVE and ARP2/3

complexes. *Proceedings of the National Academy of Sciences, USA* **105**, 4044–4049.

**Baxter-Burrell A, Yang ZB, Springer PS, Bailey-Serres J.** 2002. RopGAP4-dependent Rop GTPase rheostat control of *Arabidopsis* oxygen deprivation tolerance. *Science* **296**, 2026–2028.

**Benková E, Michniewicz M, Sauer M, Teichmann T, Seifertová D, Jürgens G, Friml J.** 2003. Local, efflux-dependent auxin gradients as a common module for plant organ formation. *Cell* **115**, 591–602.

**Berken A, Thomas C, Wittinghofer A.** 2005. A new family of RhoGEFs activates the Rop molecular switch in plants. *Nature* **436**, 1176–1180.

**Bischoff F, Vahlkamp L, Molendijk A, Palme K.** 2000. Localization of AtROP4 and AtROP6 and interaction with the guanine nucleotide dissociation inhibitor AtRhoGDI1 from *Arabidopsis*. *Plant Molecular Biology* **42**, 515–530.

**Boudsocq M, Willmann MR, McCormack M, Lee H, Shan LB, He P, Bush J, Cheng SH, Sheen J.** 2010. Differential innate immune signalling via Ca<sup>2+</sup> sensor protein kinases. *Nature* **464**, 418–422.

**Boulter E, Garcia-Mata R, Guilluy C, Dubash A, Rossi G, Brennwald PJ, Burrige K.** 2010. Regulation of Rho GTPase crosstalk, degradation and activity by RhoGDI1. *Nature Cell Biology* **12**, 477–483.

**Carol RJ, Takeda S, Linstead P, Durrant MC, Kakesova H, Derbyshire P, Drea S, Zarsky V, Dolan L.** 2005. A RhoGDP dissociation inhibitor spatially regulates growth in root hair cells. *Nature* **438**, 1013–1016.

**Chen X, Wu D, Zhao Y, Wong BHC, Guo L.** 2011. Increasing phosphoproteome coverage and identification of phosphorylation motifs through combination of different HPLC fractionation methods. *Journal of Chromatography B* **879**, 25–34.

**Cheng SH, Willmann MR, Chen HC, Sheen J.** 2002. Calcium signaling through protein kinases. The *Arabidopsis* calcium-dependent protein kinase gene family. *Plant Physiology* **129**, 469–485.

**DerMardirossian C, Schnellzer A, Bokoch GM.** 2004. Phosphorylation of RhoGDI by Pak1 mediates dissociation of Rac GTPase. *Molecular Cell* **15**, 117–127.

**Dransart E, Olofsson B, Cherfils J.** 2005. RhoGDIs revisited: novel roles in Rho regulation. *Traffic* **6**, 957–966.

**Engstrom EM, Ehrhardt DW, Mitra RM, Long SR.** 2002. Pharmacological analysis of nod factor-induced calcium spiking in *Medicago truncatula*. Evidence for the requirement of type IIA calcium pumps and phosphoinositide signaling. *Plant Physiology* **128**, 1390–1401.

**Fu Y, Gu Y, Zheng ZL, Wasteneys G, Yang ZB.** 2005. *Arabidopsis* interdigitating cell growth requires two antagonistic pathways with opposing action on cell morphogenesis. *Cell* **120**, 687–700.

**Fu Y, Li H, Yang ZB.** 2002. The ROP2 GTPase controls the formation of cortical fine F-actin and the early phase of directional cell expansion during *Arabidopsis* organogenesis. *The Plant Cell* **14**, 777–794.

- Fu Y, Wu G, Yang ZB.** 2001. Rop GTPase-dependent dynamics of tip-localized F-actin controls tip growth in pollen tubes. *Journal of Cell Biology* **152**, 1019–1032.
- Fu Y, Xu TD, Zhu L, Wen MZ, Yang ZB.** 2009. A ROP GTPase signaling pathway controls cortical microtubule ordering and cell expansion in *Arabidopsis*. *Current Biology* **19**, 1827–1832.
- Fu Y, Yang ZB.** 2001. Rop GTPase: a master switch of cell polarity development in plants. *Trends in Plant Science* **6**, 545–547.
- Garcia-Mata R, Boulter E, BurrIDGE K.** 2011. The ‘invisible hand’: regulation of RHO GTPases by RHOGDIs. *Nature Reviews Molecular Cell Biology* **12**, 493–504.
- Geiger D, Scherzer S, Mumm P, et al.** 2010. Guard cell anion channel SLAC1 is regulated by CDPK protein kinases with distinct  $Ca^{2+}$  affinities. *Proceedings of the National Academy of Sciences, USA* **107**, 8023–8028.
- Gu Y, Li SD, Lord EM, Yang ZB.** 2006. Members of a novel class of *Arabidopsis* Rho guanine nucleotide exchange factors control rho GTPase-dependent polar growth. *The Plant Cell* **18**, 366–381.
- Hwang JU, Vernoud V, Szumlanski A, Nielsen E, Yang ZB.** 2008. A tip-localized RhoGAP controls cell polarity by globally inhibiting Rho GTPase at the cell apex. *Current Biology* **18**, 1907–1916.
- Hwang JU, Wu G, Yan A, Lee YJ, Grierson CS, Yang ZB.** 2010. Pollen-tube tip growth requires a balance of lateral propagation and global inhibition of Rho-family GTPase activity. *Journal of Cell Science* **123**, 340–350.
- Ivashuta S, Liu JY, Liu JQ, Lohar DP, Haridas S, Bucciarelli B, VandenBosch KA, Vance CP, Harrison MJ, Gantt JS.** 2005. RNA interference identifies a calcium-dependent protein kinase involved in *Medicago truncatula* root development. *The Plant Cell* **17**, 2911–2921.
- Jaillais Y, Santambrogio M, Rozier F, Fobis-Loisy I, Miège C, Gaude T.** 2007. The retromer protein VPS29 links cell polarity and organ initiation in plants. *Cell* **130**, 1057–1070.
- Kaothien P, Ok SH, Shuai B, Wengier D, Cotter R, Kelley D, Kiriakopoulos S, Muschiatti J, McCormick S.** 2005. Kinase partner protein interacts with the LePRK1 and LePRK2 receptor kinases and plays a role in polarized pollen tube growth. *The Plant Journal* **42**, 492–503.
- Kaplan B, Davydov O, Knight H, Galon Y, Knight MR, Fluhr R, Fromm H.** 2006. Rapid transcriptome changes induced by cytosolic  $Ca^{2+}$  transients reveal ABRE-related sequences as  $Ca^{2+}$ -responsive cis elements in *Arabidopsis*. *The Plant Cell* **18**, 2733–2748.
- Klahre U, Becker C, Schmitt AC, Kost B.** 2006. Nt-RhoGDI2 regulates Rac/Rop signaling and polar cell growth in tobacco pollen tubes. *The Plant Journal* **46**, 1018–1031.
- Klahre U, Kost B.** 2006. Tobacco RhoGTPase ACTIVATING PROTEIN1 spatially restricts signaling of RAC/Rop to the apex of pollen tubes. *The Plant Cell* **18**, 3033–3046.
- Kost B.** 2008. Spatial control of Rho (Rac-Rop) signaling in tip-growing plant cells. *Trends in Cell Biology* **18**, 119–127.
- Kraynov VS, Chamberlain C, Bokoch GM, Schwartz MA, Slabaugh S, Hahn KM.** 2000. Localized Rac activation dynamics visualized in living cells. *Science* **290**, 333–337.
- Lavy M, Bloch D, Hazak O, Gutman I, Poraty L, Sorek N, Sternberg H, Yalovsky S.** 2007. A novel ROP/RAC effector links cell polarity, root-meristem maintenance, and vesicle trafficking. *Current Biology* **17**, 947–952.
- Le J, Mallery EL, Zhang CH, Brankle S, Szymanski DB.** 2006. *Arabidopsis* BRICK1/HSPC300 is an essential WAVE-complex subunit that selectively stabilizes the Arp2/3 activator SCAR2. *Current Biology* **16**, 895–901.
- Lemichez E, Wu Y, Sanchez JP, Mettouchi A, Mathur J, Chua NH.** 2001. Inactivation of AtRac1 by abscisic acid is essential for stomatal closure. *Genes and Development* **15**, 1808–1816.
- Mehlmer N, Wurzinger B, Stael S, Hofmann-Rodrigues D, Csaszar E, Pfister B, Bayer R, Teige M.** 2010. The  $Ca^{2+}$ -dependent protein kinase CPK3 is required for MAPK-independent salt-stress acclimation in *Arabidopsis*. *The Plant Journal* **63**, 484–498.
- Mori IC, Murata Y, Yang YZ, et al.** 2006. CDPKs CPK6 and CPK3 function in ABA regulation of guard cell S-type anion- and  $Ca^{2+}$ -permeable channels and stomatal closure. *PLoS Biology* **4**, 1749–1762.
- Myers C, Romanowsky SM, Barron YD, Garg S, Azuse CL, Curran A, Davis RM, Hatton J, Harmon AC, Harper JF.** 2009. Calcium-dependent protein kinases regulate polarized tip growth in pollen tubes. *The Plant Journal* **59**, 528–539.
- Romeis T, Piedras P, Jones JDG.** 2000. Resistance gene-dependent activation of a calcium-dependent protein kinase in the plant defense response. *The Plant Cell* **12**, 803–815.
- Sorek N, Gutman O, Bar E, et al.** 2011. Differential effects of prenylation and s-acylation on type I and II ROPS membrane interaction and function. *Plant Physiology* **155**, 706–720.
- Tao LZ, Cheung AY, Nibau C, Wu HM.** 2005. RAC GTPases in tobacco and *Arabidopsis* mediate auxin-induced formation of proteolytically active nuclear protein bodies that contain AUX/IAA proteins. *The Plant Cell* **17**, 2369–2383.
- Tao LZ, Cheung AY, Wu HM.** 2002. Plant Rac-like GTPases are activated by auxin and mediate auxin-responsive gene expression. *The Plant Cell* **14**, 2745–2760.
- Walter M, Chaban C, Schutze K, et al.** 2004. Visualization of protein interactions in living plant cells using bimolecular fluorescence complementation. *The Plant Journal* **40**, 428–438.
- Wang YP, Li L, Ye TT, Zhao SJ, Liu Z, Feng YQ, Wu Y.** 2011. Cytokinin antagonizes ABA suppression to seed germination of *Arabidopsis* by downregulating ABI5 expression. *The Plant Journal* **68**, 249–261.
- Wong HL, Pinontoan R, Hayashi K, et al.** 2007. Regulation of rice NADPH oxidase by binding of Rac GTPase to its N-terminal extension. *The Plant Cell* **19**, 4022–4034.
- Wu G, Gu Y, Li SD, Yang ZB.** 2001. A genome-wide analysis of *Arabidopsis* Rop-interactive CRIB motif-containing proteins that act as Rop GTPase targets. *The Plant Cell* **13**, 2841–2856.
- Wu G, Li H, Yang ZB.** 2000. *Arabidopsis* RopGAPs are a novel family of Rho GTPase-activating proteins that require the Cdc42/Rac-interactive binding motif for Rop-specific GTPase stimulation. *Plant Physiology* **124**, 1625–1636.



**Xu TD, Wen MZ, Nagawa S, et al.** 2010. Cell surface- and Rho GTPase-based auxin signaling controls cellular interdigitation in *Arabidopsis*. *Cell* **143**, 99–110.

**Yang ZB.** 2008. Cell polarity signaling in *Arabidopsis*. *Annual Review of Cell and Developmental Biology* **24**, 551–575.

**Yoon GM, Dowd PE, Gilroy S, McCubbin AG.** 2006. Calcium-dependent protein kinase isoforms in *Petunia* have distinct functions in pollen tube growth, including regulating polarity. *The Plant Cell* **18**, 867–878.

**Yoshizaki H, Ohba Y, Kurokawa K, Itoh RE, Nakamura T, Mochizuki N, Nagashima K, Matsuda M.** 2003. Activity of Rho-family GTPases during cell division as visualized with FRET-based probes. *Journal of Cell Biology* **162**, 223–232.

**Zhang C, Halsey LE, Szymanski DB.** 2011. The development and geometry of shape change in *Arabidopsis thaliana* cotyledon pavement cells. *BMC Plant Biology* **11**, 27.